We are IntechOpen, the world's leading publisher of Open Access books Built by scientists, for scientists

6,900
Open access books available

185,000
International authors and editors

200M
Downloads

154
Countries delivered to

Our authors are among the
TOP 1%
most cited scientists

12.2%
Contributors from top 500 universities

WEB OF SCIENCE™

Selection of our books indexed in the Book Citation Index
in Web of Science™ Core Collection (BKCI)

Interested in publishing with us?
Contact book.department@intechopen.com

Substrate Effects of Noble Metal Nanostructures Prepared by Sputtering

Alena Reznickova, Ondrej Kvitek, Dominik Fajstavr, Nikola Slavikova and Vaclav Svorcik

Additional information is available at the end of the chapter

http://dx.doi.org/10.5772/intechopen.71340

Abstract

Cathode sputtering is a well-established technique for preparation of metal nanostructures. However, the substrate properties are very important in this process. On glass substrates, there is a difficulty with poor adhesion of the metal layers, but thanks to this, metal nanostructures can be produced using solid state dewetting process. Thin metal films on polymer substrates are strongly influenced by the surface properties of the polymers, which originate in the method of their preparation. A recent focus is direct sputtering of metal nanoparticles (NPs) into liquid substrates and their characterizations and applications. Polyethylene glycol (PEG) is one of the most commonly used liquid, which provides "stealth" character to nanostructures. Recent results in this area are reviewed in this chapter. PEGylated NPs could find application in drug delivery systems, therapy, imaging, biosensing, and tissue regeneration.

Keywords: sputtering, noble metal, polymer, glass, adhesion, dewetting, thin film, polyethylene glycol, glycerol, nanoparticles, colloidal stability

1. Introduction

Cathode sputtering as a method of thin noble metal film preparation has been recently extended to a much wider variety of applications not only in electronics industry, but also in, for example, medicine or biotechnology. It has become an important technology for material processing for technologies such as multifunctional materials or nanoelectromechanical systems. A special attention in the process must be paid to the underlying substrate, which is the key factor in determining properties of the material. The material types used for substrates can be basically divided into metals, glass and ceramics, and polymers. While

metals as substrates for noble metal films possess some advantageous properties (such as good adhesion), the real potential of thin film structures on substrates stems from the different properties of each component of the material. In many cases, an insulating material is needed for the material to be functional. Of the insulating substrates, the most significant are glass and polymer substrates, which will be discussed further in this chapter.

Completely new possibilities have opened up with sputtering of noble metals onto liquid substrates. Under appropriate conditions, the use of liquid capture media leads to direct preparation of metal nanoparticles, which show some unique possibilities compared to those prepared by other methods. Ionic liquids (ILs) are one of the most commonly used capturing media for direct metal sputtering. Their significantly less toxic alternatives are vegetable oils. The main condition for selecting a suitable liquid substrate is sufficiently low vapor pressure in vacuum. Polyethylene glycol is one of the most used NP stabilizing polymers. Therefore, the use of liquid substrates for sputtering deposition has recently become a highly studied topic.

2. Cathode sputtering

When high-energy ions impact on a solid surface, the atoms of the surface material are ejected from the surface and spread into the vicinity. The phenomenon is called sputtering and is a widespread method used for deposition of thin films and ion etching.

Three main types of sputtering systems in practical use are: direct current (DC) sputtering, radio-frequency (RF) sputtering, and magnetron sputtering. Among these, the simplest is the DC sputtering system. It consists of two planar electrodes placed in a vacuum chamber. A sheet of the material to be deposited (target) is placed on one of the electrodes (cathode). Substrates to be covered with the target material are positioned on the anode. After a sufficient vacuum is established, an inert work gas (usually Ar at pressure of about 1–5 Pa) is introduced and high voltage is brought to the electrodes. The working gas is then ionized due to collisions with electrons and plasma is formed in the chamber. The generated Ar ions then collide with the cathode resulting in deposition of the target material on the substrates.

Two major drawbacks of the basic direct current are slow deposition rate and overheating and structural damage of the substrate due to extensive electron bombardment. Therefore, magnetic field is often introduced in magnetron sputtering systems in such a way it forces electrons to follow spiral trajectories, which lead to more ionizing collisions. This allows use of lower sputtering pressure and leads to higher sputtering yield. Furthermore, only electrically conductive materials can be deposited by DC sputtering. For deposition of insulating materials, the RF sputtering technique was introduced.

To control the sputtering rate, energy of the sputtered atoms and, in turn, the characteristics of the prepared films, discharge voltage, current, distance between the target and the substrate, and the work gas pressure can be manipulated. Another important parameter is the vacuum and work gas purity. Residual oxygen remaining in the sputtering chamber leads to oxidation

of the deposited material. Noble metals—great electrical conductors resistant to oxidation and other chemical reactions—are ideal materials to be used for thin film preparation by the DC diode sputtering method. More in-depth studies on the topic of cathode sputtering can be found in the literature [1–5].

3. Sputtering of noble metals onto solid insulating substrates

3.1. Glass substrates

Glass is an often-used substrate for preparation of thin metal films for electronics and optics. Its surface can be prepared with a very low roughness, is therefore able to support films with thickness as low as several nanometers and enables preparation of very delicate nanostructures. A downside of a glass substrate for sputtering of Au films is a poor adhesion of the films to the substrate. Due to surface morphology and chemical properties of the glass, the surface free energy between Au, and the glass is too high. The as-sputtered continuous films are therefore metastable. A lot of effort is therefore made to improve the adhesion between the substrates and the metal films, but the metastable nature of the films also enables advantageous preparation of isolated island nanostructure. While continuous Au films are necessary for preparation of reliable and durable metallization in electronics, the nanostructures can be used in construction of sensor devices due to their specific optical properties.

3.1.1. Adhesion of Au layers

The adhesion is defined as the energy required to create free surfaces from the bonded materials. In a practical arrangement, the interfacial toughness involves prevention of initiation and propagation of cracks, plastic deformation, and friction in the thin film-substrate system [6]. To achieve good adhesion, a strong bond between the film and the substrate must be established and parameters such as crystal orientation, contact area and, chemical affinity play very important roles. Typical methods to improve adhesion between noble metal film and glass substrate include preparation of interlayers of more reactive metals (e.g., Cr or Ti) [7–10], irradiation by energetic ion beams [11–13], thermal conditioning [14], or chemical modification of the substrate surface [15, 16], though each method has certain limitations. The metal interlayers create alloys with the thin film, changing its optical properties [17]. Ion irradiation leads to contamination of the substrate with material of the vacuum chamber and implantation of the ions in the substrate. Thermal processes lead to compromising homogeneity of very thin films. The chemical modifications of the substrate lead to introduction of more substances in the system worsening reproducibility of the production of the material.

The most common approaches to measure adhesion of a film to the substrate involve peeling of the films with adhesive tapes and various arrangements of a solid point penetrating the thin film [6]. The solid point methods include indentation measurements, which can be used to evaluate adhesion of brittle and weakly bonded layers, and scratch. The adhesion of the thin film is determined by critical loads at which some type of failure of the film-substrate

system begins. The adhesion is usually evaluated in optical microscope or by acoustic emission or friction force [18]. Quantitative evaluation of the interfacial toughness from the scratch test is difficult though, but it is still very useful when comparing adhesion of films deposited under different conditions [19, 20].

3.1.2. Solid state dewetting

Thin metal films on glass substrates undergo a morphology transformation upon annealing. The sputtering deposition is accomplished at relatively low substrate temperatures and the films grow too fast for the atoms to occupy spots with the lowest energy. Therefore, the as-deposited metal layers are in a metastable state. Annealing then leads to transformation of thin film structure from continuous layers to island-like structure. This process is called solid state dewetting. The cleavage of the metal layer then often manifests in the absorption spectrum of the material, where bands connected to localized surface plasmon resonance arise. This phenomenon can be observed as a change of color of the metal film (**Figure 1**).

The dewetting is then realized at elevated temperature by diffusion of the metal atoms over the substrate in solid state, without actual phase transformation. The driving force of the process is reaching the equilibrium state with the minimum surface free energy of the metal-glass interface. The equilibrium state is defined by the interfacial energies between the metal, substrate, and the surrounding atmosphere, and it is described by the Young equation (**Figure 2**). If the surface energy of the gas-substrate interface is higher than the sum of the surface energies of substrate-metal and metal-gas interfaces, then the equilibrium state is a planar film of metal over the substrate. In most cases, however, when the substrate is of a very different nature from the film, the surface energy of the gas-substrate interface is lower than the sum and the dewetting takes place during the annealing [21–23].

On glass substrates, the dewetting of Au thin films occurs at temperatures as low as about 300°C, well below the melting temperature. Evolution of island-like structure was observed after annealing for 1 h duration, with optical and electrical properties of the material dramatically changing due to the alteration of the nanostructure [24, 25]. Later, it was found that the process is gradual and longer annealing times lead to further evolution of the structure at the
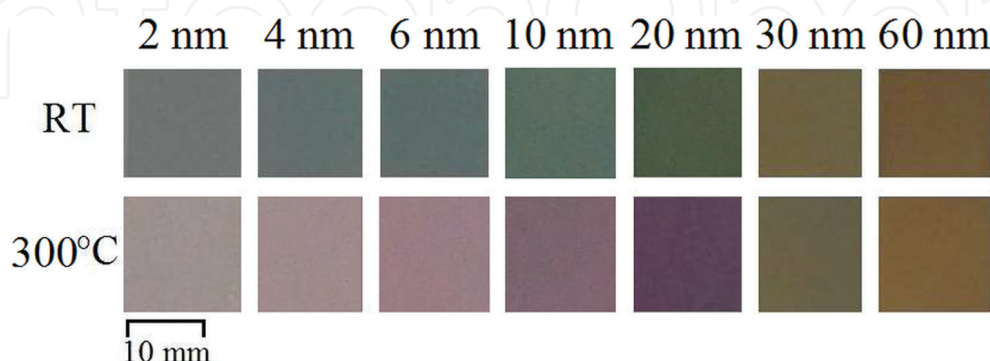

Figure 1. Photographs of 2–60 nm thin Au films sputtered on glass substrates at room temperature (RT) and after annealing at 300°C for 1 h. The distinctive color change illustrates formation of the island-like structure and the manifestation of localized surface plasmon resonance.
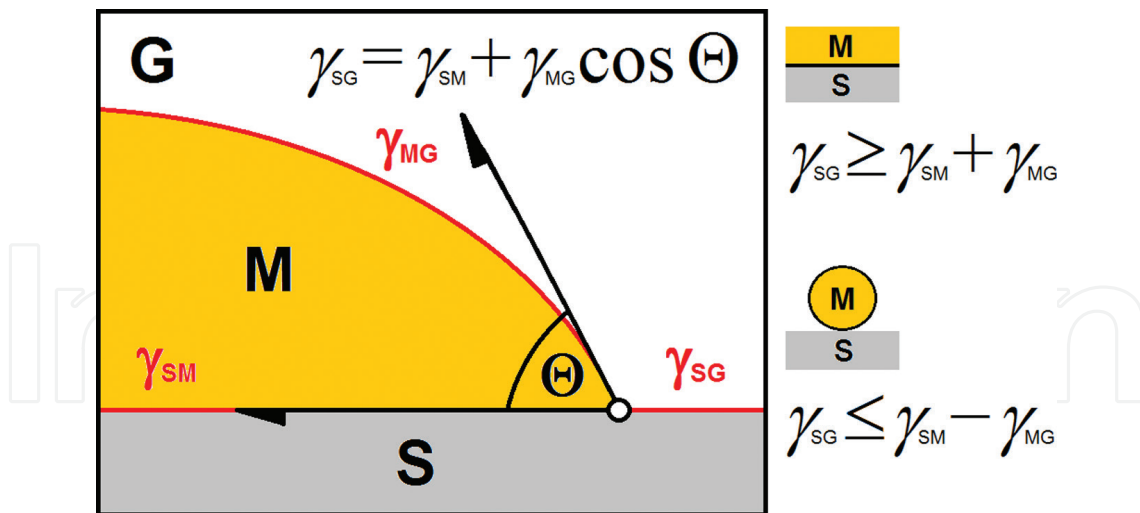
Figure 2. Illustration of the solid state dewetting in substrate (S), metal film (M), and surrounding atmosphere (G) system. The contact angle Θ between the substrate and the metal in the equilibrium state is governed by the energies of the interfaces according to the Young law. The conditions for continuous layer and total dewetting are on the right.

same temperature [26]. The dependence of the process on the surrounding atmosphere was proven by annealing of the layers in vacuum. The vacuum annealed layers tend to be more stable and the surface diffusion of the Au is somewhat slower [27]. The forming Au nanostructures were used as sensitive material for detection of vapors of organic solvents due to their specific optical properties. This is possible due to the isolated island nanostructure supporting localized surface plasmon resonance, which is strongly dependent on the refractive index of the surrounding atmosphere [28].

3.2. Polymer substrates

Due to the demand for elastic electronics for displays [29], flexible solar cells, [30] and electronic textiles [31], materials consisting of thin metal films on polymer substrates have become a highly studied subject recently. In a practical application, it is necessary to assemble stable components so the devices have the required endurance.

Compared to glass, the surface of polymers has usually higher roughness, but depending on the specific polymer, the roughness can vary a lot. Due to this fact, the morphology of film sputtered on polymers is very dependent on the surface structure of the polymer. Surface structure of substrates is formed during the preparation of the polymer foil (e.g., extrusion, casting of a solution or melted polymer, rolling, and blowing). Chemical and physical properties often govern the method that can be used to prepare a sheet the polymer—for example, sheets of polytetrafluoroethylene are prepared by cutting a block of the polymer, because it cannot be mechanically formed after its polymerization [32]. The character of functional groups on the polymer chain can also have a significant impact on the surface morphology, since it determines the polymer crystallinity [33]. This effect can be observed during annealing of the polymer. When exceeding temperatures of secondary phase transitions of the surface morphology can be significantly altered—at temperatures over the glass transition point

(T_g), polymer chain segments are enabled to shift which leads to surface recrystallization. With exceeding the melting temperature (T_m), the strain in the bulk of the polymer relaxes and a completely new surface morphology are formed [32]. The surface structure of different polymers therefore varies significantly and cannot be manipulated as precisely as the surface structure of crystalline materials.

An example of polymer substrates with very different surface morphologies are polyimide (PI) and polyetheretherketone (PEEK). The polymers were used as substrates for thin Au layer deposition and subsequently annealed. In the case of the PEEK substrate, the T_g was exceeded during annealing and the structure of the substrate surface was significantly disrupted leading to cleavage of the overlaying Au layer and changes of its optical properties (**Figure 3**).

The PI substrate is more thermally stable and preserves its surface structure during annealing at 300°C (**Figure 4**). Compared to the abovementioned case of glass substrate, the solid state dewetting was not observed on the polymer substrate, probably due to much better adhesion of the Au film [34]. Another thermally stable polymer substrate is polytetrafluoroethylene, which has a very rough surface structure. However, its surface structure can be manipulated, for example, by ion exposition in plasma discharge [35]. An intriguing substrate to support Au layers is poly-L-lactic acid. Samples with thin films show evolution of an interesting lamellar nanostructure during annealing at 60°C, which is caused by exposing of the polymer crystallites [36].
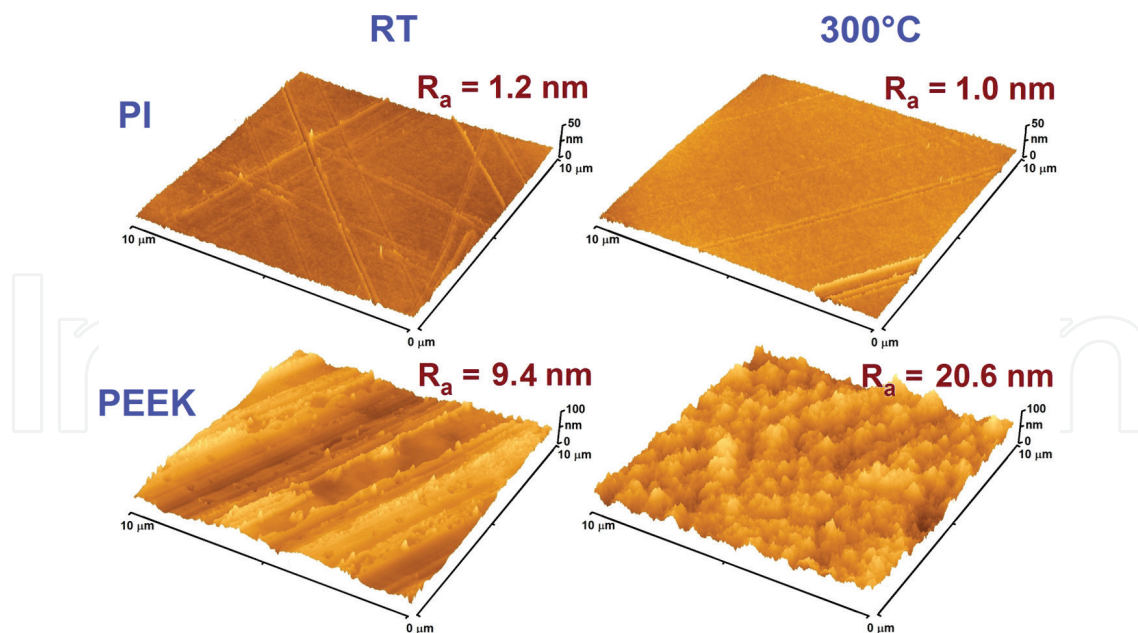

Figure 3. AFM images of the PI and PEEK substrates show significant differences of the surface structure of the polymers. While annealing of PI leads to no visible surface structure transformation, the surface of PEEK changes dramatically after annealing due to the recrystallization process. Values of surface roughness (R_a) are stated for each sample [34].
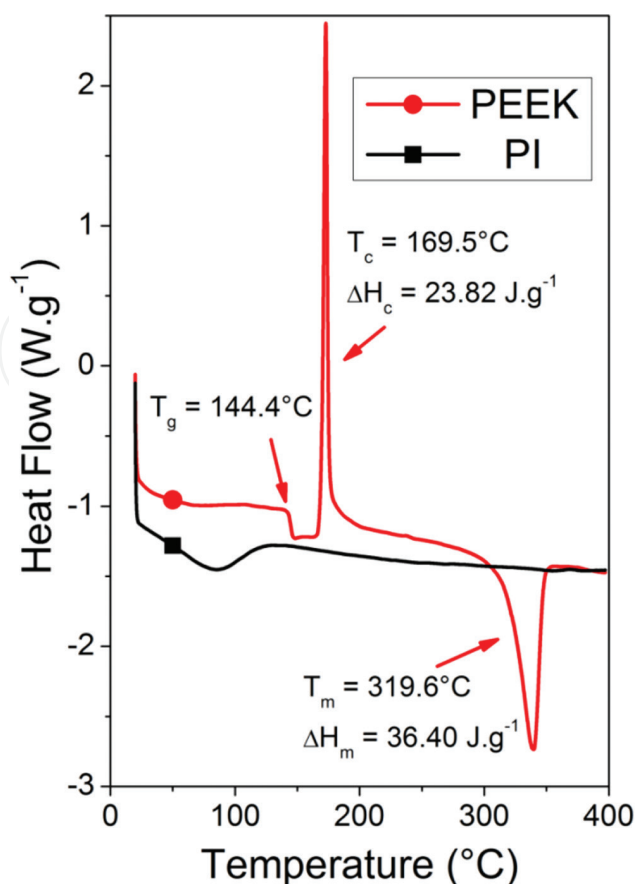
Figure 4. The DSC curves of the PI and PEEK substrates show PI is stable up to 400°C, where PEEK undergoes glass transition at ca. 144°C, then recrystallization takes place at around 170°C and it melts at about 320°C [34].

4. Sputtering of noble metals onto liquid substrates

In this part of the chapter, synthesis, properties, stability, and applications of noble metals sputtered directly into liquid substrates will be discussed. Metal nanoparticles (MNPs) have broad spectrum of applications, from electronics and catalysis to drug carriers and bio-imaging. Gold NPs (Au NPs), in particular, are widely used because of their unique properties such as size, shape, optical properties, and low toxicity [37]. NPs can be prepared by either chemical (Mie, Turkevich, Brust-Schiffrin, etc., methods) [38–40] or physical route (physical vapor deposition, laser ablation, and γ irradiation) [3, 41, 42]. The size, shape, and geometry of the NPs are strongly dependent on the employed method. Chemical synthesis offers advantages in simplicity of NP size and shape control, which enables preparation of NPs with required properties for specific application. Downside of this method is generation of harmful products and NPs with limited purity. On the other hand, the physical methods are very clean and the purity of the NPs synthesized is the same as the bulk material. In 1996 radiofrequency, sputtering of Ag NPs into a liquid substrate (silicone oil) was performed for the first time [3, 43]. However, silicone oil proved to be a suboptimal capping agent and

thus the synthesized NPs were not sufficiently stable. After 10 years of experiments, in 2006, researchers started to use ionic liquids (ILs) as liquid substrates for preparation of noble metal nanoparticles. Apart from the ILs, there are other liquid substrates, which are suitable for preparation of NPs by physical vapor deposition (i.e., sputtering). The main condition for selecting a suitable liquid substrate is sufficiently low vapor pressure in vacuum [44]. Vegetable oils [45], liquid polyethylene glycol [46, 47], molten 6-mercaptohexyltrimethylammonium bromide [48], and glycerol were used for preparation of MNPs [49]. For example, Siegel et al. demonstrated that by sputtering of various noble metals spherical NPs of different sizes can be prepared: 6.1 ± 1.0 nm for Au, 4.2 ± 0.9 nm for Ag, 2.5 ± 0.6 nm for Pd, and 1.8 ± 0.4 nm for Pt [50]. Polyethylene glycol (PEG) is one of the most commonly used stabilizing agents. It is a neutral amphiphilic polymer that gives "stealth" character to nanostructures. PEGylation of NPs is a process that introduces PEG ligands onto NPs surface. This method was introduced by Ballou et al. for the first time [51]. PEGylation generally increases circulation of NPs in blood, decreases immunity response, and slows the cleansing by the reticuloendothelial system [52]. PEG is versatile, inexpensive, and it has been approved by Food and Drug Administration (FDA) [53]. Properties of PEGylated MNPs also depend on molecular weight of the liquid PEG. Slepicka et al. prepared Au and Ag NPs by sputtering into PEG with molecular weight of 200, 400, and 600 g mol^{-1}. Since PEG-200 and PEG-600 showed lower stability during aging, only PEG-400 was used for further experiments. The prepared Au and Ag NPs were spherical with size of 7.97 ± 2.92 nm and 30–50 nm, respectively. Localized surface plasmon resonance absorption bands lied between 513 and 560 nm for Au NPs and 401–421 nm for Ag NPs [46].

4.1. Synthesis and properties of PEGylated gold nanoparticles

In this segment, results of our research for the preparation, properties, and examination of temperature and aging stability of gold nanoparticles (Au NPs) are presented. In many research papers, NPs synthesis is a multistep process consisting of many purification processes. In the first step, NPs are synthesized using a surfactant (e.g., citrate) as a stabilizing agent and, in the next step, the capping agent is exchanged with PEG molecules [54–56]. We present a simple, reproducible, environmentally friendly, low cost, and easily applicable approach of Au NPs preparation by direct sputtering of Au into a mixture of polyethylene glycol (PEG) and thiolated PEG (see **Figure 5A**). NPs consist of two components: the core and the corona, which interacts with the surrounding media (**Figure 5B**). The —OH groups of PEG create hydrogen bridges with water, which leads to formation of a solvation shell and stabilization of the NPs, preventing aggregation during dissolution. A stronger stabilization is achieved with thiol groups that have good affinity to Au. In the case of thiolated PEGs, the bond between Au and the thiol group is very strong (197.4 kJ/mol) and minimizes desorption of PEG from NP surface (**Figure 5C**) [57].

Our research group prepared Au NPs by direct sputtering for 300, 900, and 1800 s into PEG (300 s—A; 900 s—B), PEG: PEG-SH (1800 s—C), PEG: PEG-S$_2$H$_2$ (900 s—D; 300 s—E), PEG admixed with PEG-SH (300 s—F; 900 s—G) and PEG admixed with PEG-S$_2$H$_2$ (300 s—H; 900 s—I). Immediately after sputtering, the PEG with Au NPs was mixed with distilled water in the volume ratio of 1:9 (PEG: water). Molecular weights of selected polyethylene glycols
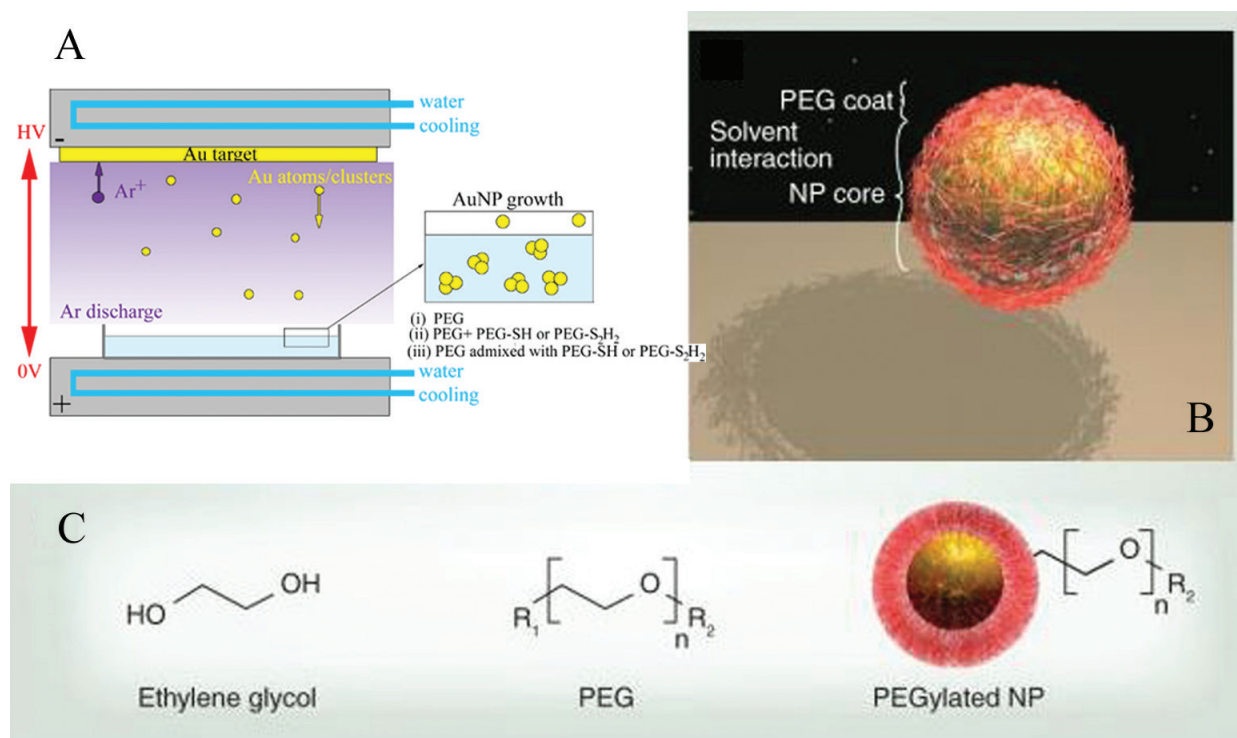
Figure 5. Schema of (A) preparation of PEGylated Au NPs by direct sputtering into liquid media of (i) PEG; (ii) PEG + PEG-SH or PEG + PEG-S$_2$H$_2$, and (iii) PEG and subsequent mixing with either PEG: PEG-SH or PEG: PEG-S$_2$H$_2$, respectively; (B) stabilization of Au NP by PEG, indicating metal core with immobilized PEG chains; (C) monomers of ethylene glycol are polymerized into PEG. PEG contains two end groups R1 linkage group and R2 terminus group, which reacts with the surrounding solvent [47].

were: 400 g mol^{-1} for PEG, 800 g mol^{-1} for PEG-SH, and 1500 g mol^{-1} for PEG-S$_2$H$_2$, respectively. The TEM images in **Figure 6** show that Au NPs were successfully prepared in all types of the capturing media. Despite the fact that the shape of Au NPs was spherical in all cases, an apparent difference in size, distribution, and concentration was detected.

The size and size distribution of individual PEGylated Au NP solutions are summarized in **Table 1** and in insets in **Figure 6**. The direct sputtering of Au atoms into pure PEG for 300 s and 900 s led to spherical NPs with an average diameter of 5.6 and 5.9 nm. TEM images show that the nanoparticles prepared under such conditions have the worst size distribution with inclination to create agglomerates (see **Figure 6A** and **B**). The Au NPs prepared in the solution of PEG-SH had average diameter of 2.9 nm. The small size of the nanoparticles can be caused by low interfacial tension of PEG-SH and high nucleation rates or by PEG-SH slowing down the growth of the Au NPs (**Figure 6C**) due to high stabilization effect of thiolated PEG [3, 58]. On top of that, these NPs have a narrower size distribution and a lower tendency to aggregate. During the stabilization of Au NPs in PEG-S$_2$H$_2$ solution, disulfide bridges are created. Due to interaction of thiol groups, the nanoparticles have higher tendency to agglomerate (**Figure 6D**). In the case of Au sputtering into PEG-S$_2$H$_2$ for 300 s, the tendency to aggregate was less apparent and the size distribution was narrower (i.e., 3.6 ± 0.6 nm, **Figure 6E**). Post-deposition addition of PEG-SH improves the homogeneity of the nanoparticles in terms of size, shape, and aggregation (**Figure 6F** and **G**) and leads
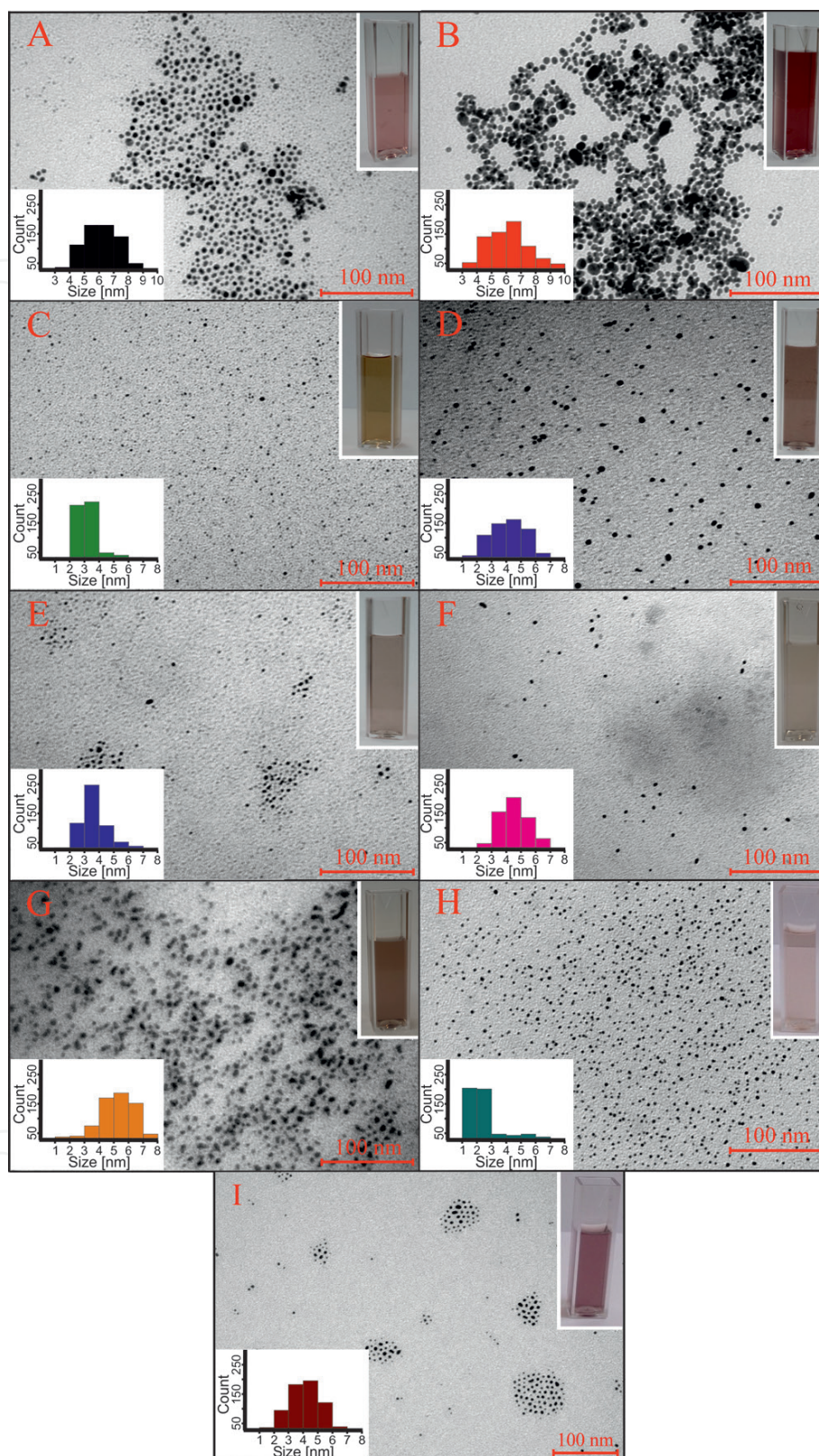
Figure 6. TEM images of Au NPs prepared by direct sputtering into PEG (300 s—A; 900 s—B), PEG: PEG-SH (1800 s—C), PEG: PEG-S$_2$H$_2$ (900 s—D; 300 s—E), PEG admixed with PEG-SH (300 s—F; 900 s—G) and PEG admixed with PEG-S$_2$H$_2$ (300 s—H; 900 s—I). Histograms of Au NPs size distribution (from TEM analysis) are shown in the inset on the left. Color of prepared PEGylated Au NPs is represented by cuvette images in insets on the right of each image [47].

to a small decrease of average NP size too (see **Table 1**). In the case of the post-deposition PEG-S$_2$H$_2$ addition (**Figure 6H**, **I** and **Table 1**) the AuNPs size decreased as well, but the agglomeration was more noticeable (**Figure 6I**). This behavior might be connected to the decrease of energy of the system after post-deposition addition of PEG-S$_2$H$_2$ compared to the energy of the system after addition of PEG-SH, and thus, the growth slowdown is more pronounced [59]. Another reason could be the different molecule weights of the used PEG-S$_2$H$_2$ and PEG-SH. Sputtering of Au into thiolated PEG or its addition leads to change of the color of the solution from dark/light red to dark/light brown (depending on concentration of the Au NPs in the solution) [47].

To confirm measured dimensions of NPs obtained from TEM, dynamic light scattering (DLS) analysis was conducted. The values of nanoparticle sizes together with polydispersity index (quantifying the degree of the size dispersion) are listed in **Table 1**. In the case of DLS, the statistical significance of designated values of particle size is much higher because all particles in a particular sample are used for the calculation (determination). The prepared colloidal solutions have mono-nodal distribution of sizes (see **Table 1**), that means, they do not contain nanoparticle aggregates, which are in good agreement with TEM results (**Figure 6**). We believe that this discrepancy is caused by the coalescence of NPs during preparation of TEM sample for the analysis. The phenomenon probably occurs during evaporation of solution on the copper grid. To assess the monodispersity of the prepared PEGylated Au NPs, we present the results of DLS analysis in the form of intensity-esteemed distribution curve of the sizes. This curve is most sensitive to presence of agglomerates, which would not be visible in the case of transformation to other types of distribution curve (volume-esteemed or number-esteemed). Another reason for discrepancy between the DLS and the TEM results is that the DLS method is not based only on hydrodynamic average of the particles themselves, but also includes the solvation shel.l [60]. Since the nanoparticles are stabilized with relatively long macromolecular chains, the detected NP sizes may be influenced by PEG corona. This is the

Sample	Au NP size (nm)		PDI
	TEM	DLS	
A	5.6 ± 1.8	9.2 ± 1.5	0.429
B	5.9 ± 0.8	8.8 ± 2.2	0.201
C	2.9 ± 0.4	3.0 ± 0.6	0.026
D	4.0 ± 1.2	4.9 ± 1.0	0.066
E	3.6 ± 0.6	4.3 ± 1.2	0.107
F	4.2 ± 0.8	5.2 ± 1.5	0.517
G	5.7 ± 1.3	7.0 ± 1.9	0.311
H	2.1 ± 0.7	4.3 ± 1.1	0.112
I	4.1 ± 1.3	6.5 ± 1.3	0.214

Table 1. Size of PEGylated Au NPs (in nm; with relative error) determined by TEM and DLS methods. Polydispersity index (PDI) of colloidal systems was determined by DLS analysis [47].

reason for not using number-esteemed averages for DLS, because the calculation for this type of results may alter the output significantly. Despite some weaknesses mentioned above, the results presented on the basis of DLS correspond well with published studies [61].

Figure 7 shows UV-Vis spectra of Au NPs sputtered into solutions of different polyethylene glycols. Comparing absorbance of each sample, significant differences in the spectra of the PEGylated Au NPs are observed. The occurrence of a singular SPR absorption peak confirms that spherical NPs are present in all colloidal PEG solutions with size ranging between 4 and 50 nm. PEGylated Au NPs prepared by sputtering for 300 s into pure PEG exhibit a narrow SPR band (at 519 nm) with the highest UV-Vis absorption. With increasing sputtering time, the SPR band tends to get wider, which is caused by the poor size distribution of NPs. The absorption also decreases, which suggests formation of sedimentation aggregates (see **Figure 6B**). In contrast, SPR bands are not observed in the spectra of Au NPs sputtered for 1800 s into PEG-SH (**Figure 7**—line C). According to literature, the peak position and absorption of the plasmon band depend on Au NPs' size and shape [59]. When the diameter of spherical Au NPs is lower than 3 nm, the plasmon band disappears [62]. Weak and broad SPR band observed for NPs stabilized with PEG-S$_2$H$_2$ (**Figure 7**—line D) might be connected to the creation of disulfide bridges, aggregation of the nanoparticles, their sedimentation and the subsequent decrease of metal concentration in the colloidal solution. The disappearance
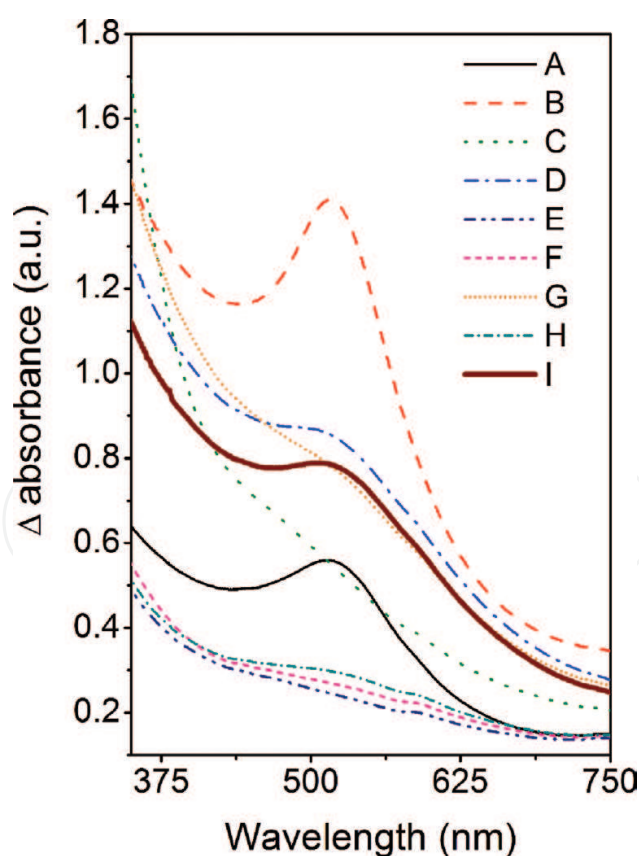

Figure 7. UV-Vis spectra of Au NPs prepared by different time of sputtering of Au into: PEG (300 s—A; 900 s—B), PEG: PEG-SH (1800 s—C), PEG: PEG-S$_2$H$_2$ (900 s—D; 300 s—E), PEG admixed with PEG-SH (300 s—F; 900 s—G) and PEG admixed with PEG-S$_2$H$_2$ (300 s—H; 900 s—I) [47].

of SPR band was noticed for Au NPs obtained by sputtering for 300 s into PEG-S$_2$H$_2$ as well as for sample C, because their size was close to 3 nm (see **Table 1**). Admixing thiolated PEG in both cases of 300 s and 900 s sputtering time leads to the disappearance of SPR bands. In the literature, the SPR absorption decrease is associated with binding of stabilizing agents containing thiol groups onto NP surface [54, 63]. Higher UV-Vis absorption of sample G is caused by the higher concentration of metal in the colloid solution. If the gold is sputtered for 300 s into PEG and the PEG-S$_2$H$_2$ is added subsequently, the prepared nanoparticles are 2.1 nm in diameter which induce the loss of the SPR band. Another possible cause is the connection of thiol groups to the Au NPs surface [54]. In the case of the gold sputtered for 900 s into pure PEG and subsequently mixed with PEG-S$_2$H$_2$, bigger nanoparticles were observed. Sputtering time of 900 s seems to be sufficient for the growth of bigger nanoparticles and, thus, the SPR band is visible in the spectrum.

Table 2 summarizes Au concentration in the solution measured by atomic absorption spectroscopy (AAS). Obtained data are in good agreement with results published by Slepicka et al.; in that, Au concentration linearly increases with the increasing sputtering time [46]. AAS confirmed results (see above) that dithiol-stabilized Au NPs are less stable aggregates and thus lower Au concentration is observed. Since these results were examined in the case of post-deposition addition of dithiols as well, we can infer that the lower concentration of Au is not connected to different liquid substrates used in the Au sputtering. With this knowledge, we are able to prepare colloids of desired NPs' size and concentration by managing the preparation conditions. Gold concentration in colloid solutions influences optical properties of the solutions such as color and UV-Vis absorption (see **Figures 6** and **7**).

4.2. Aging and temperature stability of PEGylated gold nanoparticles

For aging and temperature stability study, we have chosen samples C and D as representatives of direct Au sputtering into PEG-SH and PEG-S$_2$H$_2$, respectively. Aging and temperature stability of Au colloids was studied by UV-Vis spectroscopy (see **Figures 8** and **9**). Aging stability

Sample	c$_{Au}$ (mg l^{-1})
A	30.0
B	84.2
C	163.0
D	77.2
E	25.5
F	22.0
G	80.9
H	24.8
I	65.6

Table 2. Concentration of Au (c$_{Au}$, mg l^{-1}) in water-PEG solutions (by volume 1:9) determined by AAS spectroscopy [47].
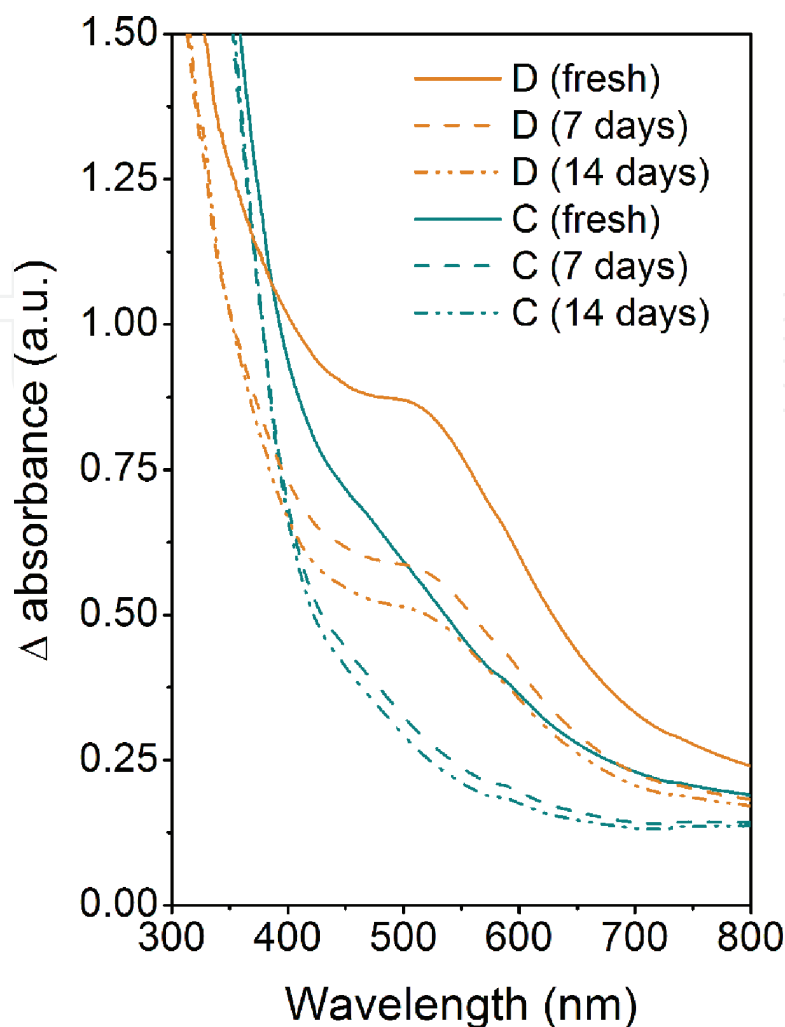
Figure 8. Aging stability (from 0 to 14 days) of Au NPs prepared by sputtering into PEG: PEG-SH (sample C) and PEG: PEG-S$_2$H$_2$ (sample D) examined by UV-Vis spectroscopy [47].

was examined in the period of 0–14 days (see **Figure 8**). **Figure 8** shows a decrease of UV-Vis absorption, which means the PEGylated Au NPs tend to slightly aggregate with aging time. Au NPs protected by PEG-SH appear to be more stable than the NPs protected by PEG-S$_2$H$_2$, since there are no significant changes in the UV-Vis absorption spectrum of those after 14 days of aging.

The progress in temperature stability of samples C and D is well documented by spectra in **Figure 9**. Immediately after the preparation of Au NPs, the samples were heated for one hour at 35, 60, 75–100°C, respectively. UV-Vis spectra measured at room temperature (RT) were used as reference. **Figure 9** shows that the post-deposition heating of colloidal solution C (Au NPs stabilized by PEG-SH) at temperature 35°C induces only a mild decrease of UV-Vis absorption, which did not change with further temperature increase. The post-sputtering heating of sample D (Au NPs protected by PEG-S$_2$H$_2$) caused a gradual decrease of UV-Vis absorption with increasing temperature. The sample D turns out to have lower temperature stability with the tendency for aggregation compared to the sample C. The results of aging and temperature stability of Au NPs with core shielded by PEG-SH molecules (sample C) are in good agreement with data published by Hatakeyama et al. [41].
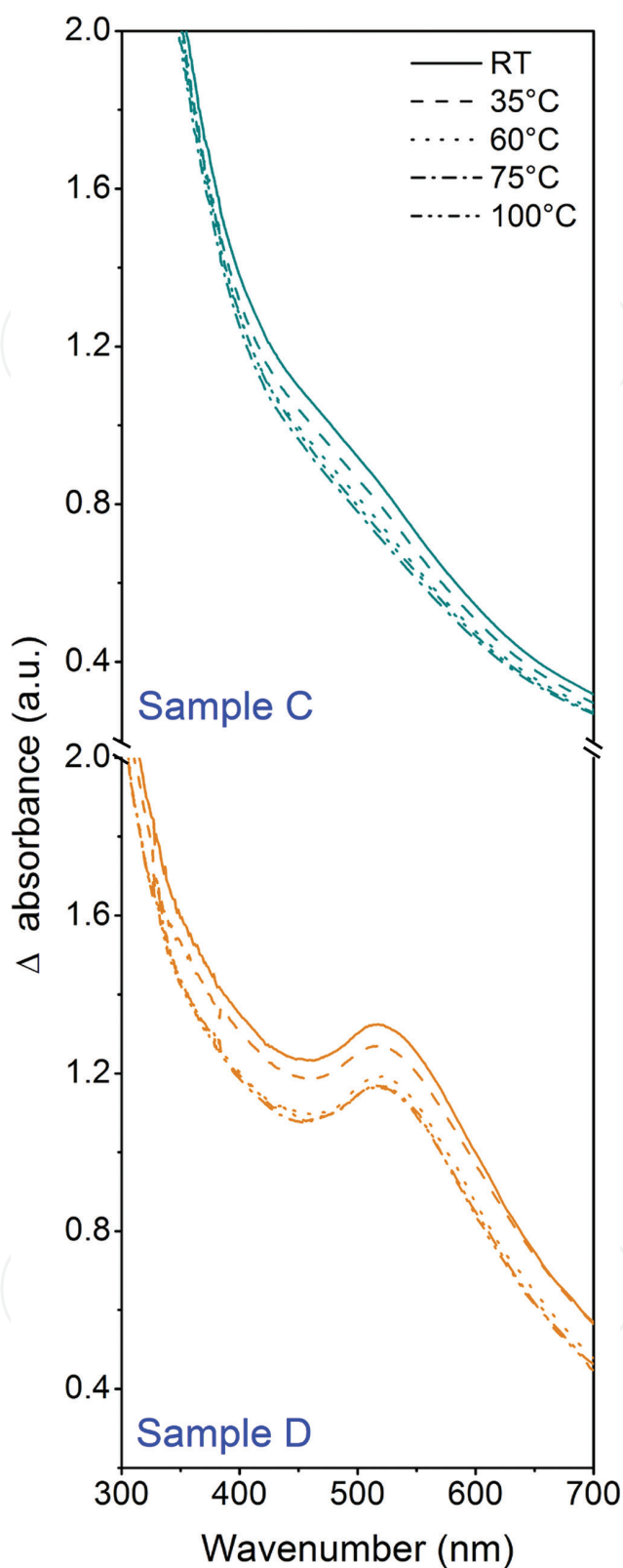
Figure 9. Temperature stability (from RT to 100°C) of Au NPs prepared by sputtering into PEG: PEG-SH (Sample C) and PEG: PEG-S$_2$H$_2$ (Sample D) examined by UV-Vis spectroscopy [47].

Hatakeyama et al. investigated the effect of temperature on the structure and growth of Au NPs prepared by sputtering method by small-angle X-ray scattering. Ionic liquid 1-buthyl-3-methylimidazolium tetrafluoroborate was used as the liquid substrate. The

liquid was heated from 20 to 80°C before sputtering. It was found that the Au NP sizes (i) are uniform at constant temperature, (ii) increase as the temperature rises, and (iii) values of W_{FWHM} (full width at half maxima of distribution curves) increase with the rising temperature. At lower temperatures (20 and 30°C), W_{FWHM} values were almost the same as d_{peak} (diameter at the peak-top of distribution curves) values. The values gradually increase and reach 40–70°C, and then increases dramatically with temperature [64].

4.3. Applications of PEGylated nanoparticles

Polyethylene glycol is one of the most used NP stabilizing polymer and the gold standard for "stealth" polymers in the emerging area of polymer-based drug carriers, gene vectors, imaging, therapeutic agents, bio-sensing, and tissue regeneration [65, 66].

Localized surface plasmon resonance (LSPR) is specific property of Au NPs that depends on particle size and distance between the particles. In the case of Au NPs, the absorption maximum connected to LSPR is between 500 and 550 nm. LSPR phenomenon is associated with oscillation of the electron gas due to excitation by incident light beam. This property puts the Au NPs to the forefront of interest in the area of biosensors technology. Creation of Au NPs aggregates invokes interparticle surface plasmon coupling, which leads to a dramatic change of color of the colloidal solution from red to blue. It also causes broadening of the surface plasmon resonance peak. Significant color change of colloids can be easily seen by the naked eye, without usage of any analytical method. Aggregation of Au NPs is extensively used in colorimetric detection of DNA, metal ions, proteins, toxins, and enzyme activity too [67, 68]. Kim et al. have found a simple procedure that can identify differences between normal and increased calcium ion (Ca^{2+}) levels in serum using calsequestrin (CSQ)-immobilized Au NPs [69, 70]. Zhang et al. successfully grafted PEG-SH onto CTAB shielded gold nanorods (Au NR) and prepared uniform monolayer of Au NRs on silicon by gradual evaporation of the residual water. This approach brings a new opportunity to prepare uniform plasmonic sensing platforms due to stability of PEGylated Au NRs in the serum [71].

Molecular imaging is associated with processes ongoing in living organisms at cellular and molecular levels. Diseases in early stage can be identified and monitored by specific molecular-imaging agents, which are very powerful method enabling a rapid and targeted treatment. Nowadays, MRI, CT, ultrasound, optical imaging, single-photon emission computed tomography (SPECT), and positron-emission tomography (PET) are the most commonly used imaging methods [72]. In contrast to other imaging agents, Au NPs offer better optical imaging properties because: (i) their light scattering effect is very strong, (ii) they are much brighter than chemical fluorophores, (iii) they resist photo-bleaching, and (iv) they can be easily spotted at low concentrations (10^{-16} M). For Au NPs-based contrast agents, the most promising imaging technique is Raman spectroscopy. Au NPs immobilized with thiolated PEG and conjugated with antibody specifically bind to the epidermal growth factor. These SERS nanoparticles for active targeting of both cancer cells and tumor xenografts were more than 200 times brighter than near-infrared-emitting quantum dots, and allowed spectroscopic detection of small tumors at a penetration depth of 1–2 cm [70]. Silvestri et al. have synthesized Au NPs

stabilized by PEG-SH and used them as CT contrast agents for *in vivo* experiments on mice. They have reported that the surface immobilization together with the small hydrodynamic diameters (3.8 nm) of the custom tailored Au NPs allowed their efficient renal cleansing, prolonged blood circulation, and stealth capability [73].

LSPR band of Au NPs leads to strong light absorption and efficient conversion of the energy into localized heat, which can be used for selective ablation of cancer cells [74]. This procedure is called plasmonic photothermal therapy (PPT). Liu et al. have shown that the multidentate PEG ligand functionalized Au NRs can be used as an effective NIR photothermal agent for tumor ablation *in vivo*. PEGylated Au NRs showed that low cytotoxicity on most mice organs *in vivo* had high efficacy of cancer cells ablation *in vitro*, accumulated in tumors preferentially and showed good stability in serum [75]. Li et al. prepared PEGylated Cu nanowires (Cu NWs) with efficient photothermal conversion (12.5%) by NIR irradiation at 808 nm and studied selective killing of cancer cells *in vitro* and effective photothermal ablation of cancer *in vivo*. The authors showed the intratumoral injection of PEGylated Cu-NWs into colon tumor-bearing mice and ensuing NIR irradiation (808 nm, 1.5 W/cm^2) for 6 min significantly raised the local temperature to >50°C, induced necrosis, and suppressed tumor growth [76]. Ruff et al. studied the effect of multivalency on the stability of NIR-absorbing Au NRs (CTAB stabilized) immobilized with mono-, bi- and tridentate PEG thiol ligands. Their PEGylation approach leads to Au NPs and Au NRs with CTAB concentration below the detection limit. Furthermore, high biocompatibility after PEGylation of both Au NPs and Au NRs was found and no significant difference in cytotoxicity against human cervical cancer cells comparing the mono-, bi- and tridentate PEGylated species was observed, which makes them suitable as biocompatible contrast agents [77].

Besides the PPT, PEGylated gold nanoparticles are very promising material for photodynamic therapy (PDT) drug delivery [78, 79]. NPs can be stabilized by steric repulsion to inhibit colloid aggregation in physiological conditions by using water-soluble PEG [80]. PEGylated Au NPs show remarkable resistance in protein adsorption due to the high degree of hydration of the randomly coiled PEG molecules [81]. According to this property, drugs carried by NPs could be shielded from being cleared/removed by the reticuloendothelial system (RES) [82]. Therefore, the blood circulation time of NPs can be prolonged. Drug distribution *in vivo* can be regulated too. Such drug carriers can preferentially accumulate in tumor sites through the leaky tumor neovasculature and do not re-enter the blood stream, which is called "enhanced permeability and retention" (EPR) effect [82]. Cheng et al. prepared PEGylated Au NPs conjugated with silicone phthalocyanine with a reversible PDT drug adsorption. It was found that the delivery mode of this system greatly improves the transport of the drug to the tumor compared to conventional drug administration [83]. Li et al. demonstrated that the 75 nm latex particles remained in rat circulation 40 times longer (from 20 min to 13 h) when immobilized with PEG larger than 5000 kDa [84]. Klibanov and Huang found that PEGylation leads to advantageous results in other drug delivery systems as well. PEGylation of liposomes improved their circulation half-life from 30 min to 5 h without increasing leakage of the liposome interior [85]. In the mid-1990s, Doxil® (liposomal delivery vehicle for doxorubicin) and Oncospar (PEG-L-asparaginase) became the first FDA approved NP therapeutics [86, 87].

5. Conclusions

Cathode sputtering is a well-established technique for the preparation of metal nanostructures. The manipulation of the deposition parameters enable formation of precisely controlled material. For the properties of the resulting material, the proper selection of substrate is necessary. For the traditional application of the thin metal films in electronics, insulating substrates are usually necessary, of which the glass and polymer substrates are the most important. In this chapter, we have discussed the problems of glass substrates in adhesion of the metal layers and possibilities of dewetting. The polymer substrates on the other hand provide better adhesion to the metals, but surface morphology effects are more pronounced. A new and perspective branch of substrates for sputtering deposition are liquids. Therefore, this chapter provides a deeper insight into the problems of direct sputtering of noble metals into liquid substrate, i.e., preparation of NPs. Basic characteristics, technology of preparation, and applications of those materials are explained. The results of the authors' team support the general overview. Direct sputtering of Au atoms onto PEG and thiol terminated PEG has led to successful formation of spherical NPs. The diameters of the prepared Au NPs ranged from 2.1 to 5.9 nm depending on the capturing medium. NPs smaller than 3 nm in diameter exhibited loss of SPR band because of the small NP size and/or attachment of thiolated PEG on the Au NPs' surface. Solution of Au NPs stabilized by PEG-SH (sample C) exhibited higher time and temperature stability compared to the solution where Au NPs were stabilized by PEG-S_2H_2 (sample D). This colloidal solution showed the best time and temperature stability with the size of Au NPs of 2.9 nm, which can have a positive effect in biomedical use and for catalysis of chemical reactions. PEGylated NPs have huge potential in biomedical applications (drug delivery, therapy, imaging, and biosensing).

Acknowledgements

Author details

Alena Reznickova*, Ondrej Kvitek, Dominik Fajstavr, Nikola Slavikova and Vaclav Svorcik

*Address all correspondence to: reznicka@vscht.cz

Department of Solid State Engineering, University of Chemistry and Technology Prague, Prague, Czech Republic

References

[1] Wasa K, Kanno I, Kotera H, editors. Handbook of Sputter Deposition Technology: Fundamentals and Applications for Functional Thin Films, Nano-Materials and MEMS. 2nd ed. Oxford: Elsevier; 2012 660 p

[2] Frey H, Khan HR, editors. Handbook of Thin Film Technology. Berlin: Springer Verlag; 2015. 380 p. DOI: 10.1007/978-3-642-05430-3

[3] Wender H, Migowski P, Feil AF, Teixeira SR, Dupont J. Sputtering deposition of nanoparticles onto liquid substrates: Recent advances. Coordination Chemistry Reviews. 2013;**257**:2468-2483. DOI: 10.1016/j.ccr.2013.01.013

[4] Maissel I, Glang R, editors. Handbook of Thin Film Technology. 1st ed. New York: McGraw-Hill; 1970 800 p

[5] McClanahan ED, Laegreid N. Production of thin films by controlled deposition of sputtered material. In: Behrisch R, Wittmaack K, editors. Sputtering by Particle Bombardment III. Berlin: Springer Verlag; 1991. p. 339-377. DOI: 10.1007/3540534288_21

[6] Volinsky AA, Moody NR, Gerberich WW. Interfacial toughness measurements for thin films on substrates. Acta Materialia. 2002;**50**:441-466. DOI: 10.1016/S1359-6454 (01)00354-8

[7] Haq KE, Behrndt KH, Kobin I. Adhesion mechanism of gold-underlayer film combinations to oxide substrates. Journal of Vacuum Science and Technology. 1969;**6**:148-152. DOI: 10.1116/1.1492648

[8] Sexton BA, Feltis BN, Davis TJ. Characterisation of gold surface plasmon resonance sensor substrates. Sensors and Actuators A. 2008;**141**:471-475. DOI: 10.1016/j.sna.2007.10.020

[9] Kim WM, Kim SH, Lee KS, Lee TS, Kim IH. Titanium nitride thin film as an adhesion layer for surface plasmon resonance sensor chips. Applied Surface Science. 2012;**261**:749-752. DOI: 10.1016/j.apsusc.2012.08.093

[10] Ito Y, Kushida K, Takeuchi H. Role of chromium sublayers in the growth of highly crystalline (111)-oriented gold-films on sapphire. Journal of Crystal Growth. 1991;**112**:427-436. DOI: 10.1016/0022-0248(91)90319-Z

[11] Jang HG, Kim KH, Han S, Choi WK, Jung HJ, Koh SK, Kim HB. Adhesion improvement between Au films and glass by 1 keV Ar+ ion irradiation. Journal of Vacuum Science and Technology A. 1997;**15**:2233-2239. DOI: 10.1116/1.580539

[12] Svorcik V, Kotal V, Blahova O, Spirkova M, Sajdl P, Hnatowicz V. Modification of surface properties of polyethylene by Ar plasma discharge. Nuclear Instruments and Methods in Physics Research Section B. 2006;**244**:365-372. DOI: 10.1016/j.nimb.2005.10.003

[13] Park JW, Pedraza AJ, Allen WR. The interface between sputter-deposited gold thin films and ion-bombarded sapphire substrates. Applied Surface Science. 1996;**103**:39-48. DOI: 10.1016/0169-4332(96)00097-9

[14] Nguyen TP, Ip J, le Rendu P, Lahmar A. Improved adhesion of gold coatings on ceramic substrates by thermal treatment. Surface and Coating Technology. 2001;**141**:108-114. DOI: 10.1016/S0257-8972(01)01165-3

[15] Mosier-Boss PA, Lieberman SH. Comparison of three methods to improve adherence of thin gold films to glass substrates and their effect on the SERS response. Applied Spectroscopy. 1999;**53**:862-873. DOI: 10.1366/0003702991947469

[16] Lahiri B, Dylewicz R, de la Rue RM, Johnson NP. Impact of titanium adhesion layers on the response of arrays of metallic split-ring resonators (SRRs). Optics Express. 2010;**18**:11202-11207. DOI: 10.1364/OE.18.011202

[17] Li X, Huang F, Curry M, Street SC, Weaver ML. Improved adhesion of Au thin films to SiOx/Si substrates by dendrimer mediation. Thin Solid Films. 2005;**473**:164-168. DOI: 10.1016/j.tsf.2004.07.080

[18] Yoshida S, Adhikari S, Gomi K, Shrestha R, Huggett D, Miyasaka C, Park I. Opto-acoustic technique to evaluate adhesion strength of thin-film systems. AIP Advances. 2012;**2**:022126. DOI: 10.1063/1.4719698

[19] Tsukamoto Y, Kuroda H, Sato A, Yamaguchi H. Microindentation adhesion tester and its application to thin-films. Thin Solid Films. 1992;**213**:220-225. DOI: 10.1016/0040-6090(92)90285-J

[20] Gerberich WW, Jungk JM, Li M, Volinsky AA, Hoehn JW, Yoder K. Length scales for the fracture of nanostructures. International Journal of Fracture. 2003;**119**:387-405. DOI: 10.1023/A:1024927812734

[21] Thompson CV. Solid-state dewetting of thin films. In: Clarke DR, editor. Annual Review of Materials Research. El Camino Way: Annual Reviews. 2012. p. 399-434. DOI: 10.1146/annurev-matsci-070511-155048

[22] Leroy F, Borowik L, Cheynis F, Almadori Y, Curiotto S, Trautmann M, Barbe JC, Muller P. How to control solid state dewetting: A short review. Surface Science Reports. 2016;**71**:391-409. DOI: 10.1016/j.surfrep.2016.03.002

[23] Kosinova A, Kovalenko O, Klinger L, Rabkin E. Mechanisms of solid-state dewetting of thin Au films in different annealing atmospheres. Acta Materialia. 2015;**83**:91-101. DOI: 10.1016/j.actamat.2014.09.049

[24] Svorcik V, Kvitek O, Lyutakov O, Siegel J, Kolska Z. Annealing of sputtered gold nanostructures. Applied Physics A: Materials Science & Processing. 2011;**102**:747-751. DOI: 10.1007/s00339-010-5977-5

[25] Svorcik V, Siegel J, Sutta P, Mistrik J, Janicek P, Worsch P, Kolska Z. Annealing of gold nanostructures sputtered on glass substrate. Applied Physics A: Materials Science & Processing. 2011;**102**:605-610. DOI: 10.1007/s00339-010-6167-1

[26] Kvitek O, Konrad P, Svorcik V. Time dependence and mechanism of Au nanostructure transformation during annealing. Functional Materials Letters. 2014;**7**:1450022. DOI: 10.1142/S1793604714500222

[27] Siegel J, Kvitek O, Lyutakov O, Reznickova A, Svorcik V. Low pressure annealing of gold nanostructures. Vacuum. 2013;**98**:100-105. DOI: 10.1016/j.vacuum.2013.03.019

[28] Tesler AB, Karakouz T, Bendikov TA, Haran G, Vaskevich A, Rubinstein I. Tunable localized plasmon transducers prepared by thermal dewetting of percolated evaporated gold films. Journal of Physical Chemistry C. 2011;**115**:24642-24652. DOI: 10.1021/jp209114j

[29] Forrest SR. The path to ubiquitous and low-cost organic electronic appliances on plastic. Nature. 2004;**428**:911-918. DOI: 10.1038/nature02498

[30] Bonderover E, Wagner S. A woven inverter circuit for e-textile applications. IEEE Electron Device Letters. 2004;**25**:295-297. DOI: 10.1109/LED.2004.826537

[31] Brabec CJ. Organic photovoltaics: Technology and market. Solar Energy Materials & Solar Cells. 2004;**83**:273-292. DOI: 10.1016/j.solmat.2004.02.030

[32] Robledo-Ortíz JR, Ramírez-Arreola DE, Rodrigue D, González-Núñez R. Blown films and ribbons extrusion. In: Saldívar-Guerra E, Vivaldo-Lima E, editors. Handbook of Polymer Synthesis, Characterization, and Processing. 1st ed. Chichester: Wiley; 2013. p. 463-472

[33] Mehmet-Alkan AA, Hay JN. The crystallinity of poly(ether ether ketone). Polymer. 1992;**33**:3527-3530. DOI: 10.1016/0032-3861(92)91116-J

[34] Kvitek O, Fajstavr D, Reznickova A, Kolska Z, Slepicka P, Svorcik V. Annealing of gold nanolayers sputtered on polyimide and polyetheretherketone. Thin Solid Films. 2016;**616**:188-196. DOI: 10.1016/j.tsf.2016.08.025

[35] Svorcik V, Siegel J, Slepicka P, Kotal V, Svorcikova J, Spirkova M. Au nanolayers deposited on polyethyleneterephtalate and polytetrafluorethylene degraded by plasma discharge. Surface and Interface Analysis. 2007;**39**:79-85. DOI: 10.1002/sia.2512

[36] Slepicka P, Fidler T, Vasina A, Svorcik V. Ripple-like structure on PLLA induced by gold deposition and thermal treatment. Materials Letters. 2012;**79**:4-6. DOI: 10.1016/j.matlet.2012.03.070

[37] Doane TL, Cheng Y, Babar A, Hill RJ, Burda C. Electrophoretic mobilities of PEGylated gold NPs. Journal of the American Chemical Society. 2010;**132**:15624-15631. DOI: 10.1021/ja1049093

[38] Mie G. Beiträge zur optik trüber medien, speziell colloidaler metallösungem. Annals of Physics. 1908;**25**:377-445. DOI: 10.1002/andp.19083300302

[39] Turkevich J, Stevenson PC, Hillier J. A study of the nucleation and growth processes in the synthesis of colloidal gold. Discussions of the Faraday Society. 1951;**11**:55-75. DOI: 10.1039/df9511100055

[40] Brust M, Walker M, Bethell D, Schiffrin DJ, Whyman R. Synthesis of thiol-derivatized gold nanoparticles in a 2-phase liquid-liquid system. Journal of the Chemical Society, Chemical Communications. 1994:801-802. DOI: 10.1039/c39940000801

[41] Hatakeyama Y, Kato J, Mukai T, Judai K, Nishikawa K. Effect of adding a thiol stabilizer on synthesis of Au nanoparticles by sputter deposition onto poly(ethylene glycol). Bulletin of the Chemical Society of Japan. 2014;**87**:773-779. DOI: 10.1246/bcsj.20140023

[42] Hori T, Nagata K, Iwase A, Hori F. Synthesis of Cu nanoparticles using gamma-ray irradiation reduction method. Japanese Journal of Applied Physics. 2014;**53**:05FC05. DOI: 10.7567/jjap.53.05fc05

[43] Ye GX, Zhang QR, Feng CM, Ge HL, Jiao ZK. Structural and electrical properties of a metallic rough-thin-film system deposited on liquid substrates. Physical Review B. 1996;**54**:14754-14757. DOI: 10.1103/PhysRevB.54.14754

[44] Wender H, Gonçalves RV, Feil AF, Migowski P, Poletto FS, Pohlmann AR, Dupont J, Teixeira SR. Sputtering onto liquids: From thin films to nanoparticles. Journal of Physical Chemistry C. 2011;**115**:16362-16367. DOI: 10.1021/jp205390d

[45] Wender H, de Oliveira LF, Feil AF, Lissner E, Migowski P, Meneghetti MR, Teixeira SR, Dupont J. Synthesis of gold nanoparticles in a biocompatible fluid from sputtering deposition onto castor oil. Chemical Communications. 2010;**46**:7019-7021. DOI: 10.1039/c0cc01353f

[46] Slepička P, Elashnikov R, Ulbrich P, Staszek M, Kolská Z, Švorčík V. Stabilization of sputtered gold and silver nanoparticles in PEG colloid solutions. Journal of Nanoparticle Research. 2015;**17**:11. DOI: 10.1007/s11051-014-2850-z

[47] Reznickova A, Slepicka P, Slavikova N, Staszek M, Svorcik V. Preparation, aging and temperature stability of PEGylated gold nanoparticles. Colloids and Surfaces A. 2017;**523**:91-97. DOI: 10.1016/j.colsurfa.2017.04.005

[48] Shishino Y, Yonezawa T, Kawai K, Nishihara H. Molten matrix sputtering synthesis of water-soluble luminescent Au nanoparticles with a large Stokes shift. Chemical Communications. 2010;**46**:7211-7213. DOI: 10.1039/c0cc01702g

[49] Siegel J, Kvítek O, Ulbrich P, Kolská Z, Slepička P, Švorčík V. Progressive approach for metal nanoparticle synthesis. Materials Letters. 2012;**89**:47-50. DOI: 10.1016/j.matlet.2012.08.048

[50] Staszek M, Siegel J, Rimpelova S, Lyutakov O, Svorcik V. Cytotoxicity of noble metal nanoparticles sputtered into glycerol. Materials Letters. 2015;**158**:351-354. DOI: 10.1016/j.matlet.2015.06.021

[51] Ballou B, Lagerholm BC, Ernst LA, Bruchez MP, Waggoner AS. Noninvasive imaging of quantum dots in mice. Bioconjugate Chemistry. 2004;**15**:79-86. DOI: 10.1021/bc034153y

[52] Liu HY, Doane TL, Cheng Y, Lu F, Srinivasan S, Zhu JJ, Burda C. Control of surface ligand density on PEGylated gold nanoparticles for optimized cancer cell uptake. Particle and Particle Systems Characterization. 2015;**32**:197-204. DOI: 10.1002/ppsc.201400067

[53] Liu GY, Luo QQ, Wang HB, Zhuang WH, Wang YB. In situ synthesis of multidentate PEGylated chitosan modified gold nanoparticles with good stability and biocompatibility. RSC Advances. 2015;**5**:70109-70116. DOI: 10.1039/c5ra11600g

[54] Abd-Elaal AA, Tawfik SM, Shaban SM. Simple one step synthesis of nonionic dithiol surfactants and their self-assembling with silver nanoparticles: Characterization, surface properties, biological activity. Applied Surface Science. 2015;**342**:144-153. DOI: 10.1016/j.apsusc.2015.03.038

[55] Gao J, Huang XY, Liu H, Zan F, Ren JC. Colloidal stability of gold nanoparticles modified with thiol compounds: Bioconjugation and application in cancer cell imaging. Langmuir. 2012;**28**:4464-4471. DOI: 10.1021/la204289k

[56] Alkilany AM, Yaseen AIB, Park J, Eller JR, Murphy CJ. Facile phase transfer of gold nanoparticles from aqueous solution to organic solvents with thiolated poly(ethylene glycol). RSC Advances. 2014;**4**:52676-52679. DOI: 10.1039/c4ra11928b

[57] Di Felice R, Selloni A. Adsorption modes of cysteine on Au (111): Thiolate, amino-thiolate, disulfide. The Journal of Chemical Physics. 2004;**120**:4906-4914. DOI: 10.1063/1.1645789

[58] Wuelfing WP, Gross SM, Miles DT, Murray RW. Nanometer gold clusters protected by surface-bound monolayers of thiolated poly(ethylene glycol) polymer electrolyte. Journal of the American Chemical Society. 1998;**120**:12696-12697. DOI: 10.1021/ja983183m

[59] Murphy CJ, Sau TK, Gole AM, Orendorff CJ, Gao J, Gou L, Hunyadi SE, Li T. Anisotropic metal nanoparticles: Synthesis, assembly, and optical applications. The Journal of Physical Chemistry. B. 2005;**109**:13857-13870. DOI: 10.1021/jp0516846

[60] Uskokovic V. Dynamic light scattering based microelectrophoresis: Main prospects and limitations. Journal of Dispersion Science and Technology. 2012;**33**:1762-1786. DOI: 10.1080/01932691.2011.625523

[61] Souza TGF, Ciminelli VST, Mohallem NDS. A comparison of TEM and DLS methods to characterize size distribution of ceramic nanoparticles. Journal of Physics: Conference Series. 2016;**733**:012039. DOI: 10.1088/1742-6596/733/1/012039

[62] Daniel MC, Astruc D. Gold nanoparticles: Assembly, supramolecular chemistry, quantum-size-related properties, and applications toward biology, catalysis, and nanotechnology. Chemical Reviews. 2004;**104**:293-346. DOI: 10.1021/cr030698+

[63] Lica GC, Zelakiewicz BS, Constantinescu M, Tong YY. Charge dependence of surface plasma resonance on 2 nm octanethiol-protected Au nanoparticles: Evidence of a free-electron system. The Journal of Physical Chemistry. B. 2004;**108**:19896-19900. DOI: 10.1021/jp045302s

[64] Hatakeyama Y, Takahashi S, Nishikawa K. Can temperature control the size of Au nanoparticles prepared in ionic liquids by the sputter deposition technique? Journal of Physical Chemistry C. 2010;**114**:11098-11102. DOI: 10.1021/jp102763n

[65] Knop K, Hoogenboom R, Fischer D, Schubert US. Poly(ethylene glycol) in drug delivery: Pros and cons as well as potential alternatives. Angewandte Chemie (International Ed. in English). 2006;**49**:6288-6308. DOI: 10.1002/anie.200902672

[66] Encabo-Berzosa MD, Sancho-Albero M, Crespo A, Andreu V, Sebastian V, Irusta S, Arruebo M, Martín-Duque P, Santamaria S. The effect of PEGylated hollow gold nanoparticles on stem cell migration: Potential application in tissue regeneration. Nanoscale. 2017;**9**:9848-9858. DOI: 10.1039/c7nr01853c

[67] Slocik JM, Zabinski JS, Phillips DM, Naik RR. Colorimetric response of peptide-functionalized gold nanoparticles to metal ions. Small. 2008;**4**:548-551. DOI: 10.1002/smll.200700920

[68] Zhao WA, Chiuman W, Lam JCF, Brook MA, Li YF. Simple and rapid colorimetric enzyme sensing assays using non-crosslinking gold nanoparticle aggregation. Chemical Communications. 2007;**36**:3279-3231. DOI: 10.1039/b705335e

[69] Kim S, Park JW, Kim D, Kim D, Lee IH, Jon S. Bioinspired colorimetric detection of calcium(II) ions in serum using calsequestrin-functionalized gold nanoparticles. Angewandte Chemie International Edition. 2009;**48**:4138-4141. DOI: 10.1002/anie.200900071

[70] Kim D, Jon S. Gold nanoparticles in image-guided cancer therapy. Inorganica Chimica Acta. 2012;**393**:154-164. DOI: 10.1016/j.ica.2012.07.001

[71] Zhang Z, Lin MS. Fast loading of PEG–SH on CTAB-protected gold nanorods. RSC Advances. 2014;**4**:17760-17767. DOI: 10.1039/c3ra48061e

[72] Sharma P, Brown S, Walter G, Santra S, Moudgil B. Nanoparticles for bioimaging. Advances in Colloid and Interface Science. 2006;**123**:471-485. DOI: 10.1016/j.cis.2006.05.026

[73] Silvestri A, Polito L, Bellani G, Zambelli V, Jumde RP, Psaro R, Evangelisti C. Gold nanoparticles obtained by aqueous digestive ripening: Their application as X-ray contrast agents. Journal of Colloid and Interface Science. 2015;**439**:28-33. DOI: 10.1016/j.jcis.2014.10.025

[74] Huang XH, Jain PK, El-Sayed IH, El-Sayed MA. Plasmonic photothermal therapy (PPTT) using gold nanoparticles. Lasers in Medical Science. 2008;**23**:217-228. DOI: 10.1007/s10103-007-0470-x

[75] Liu X, Huang N, Li H, Wang H, Jing Q, Ji J. Multidentate polyethylene glycol modified gold Nanorods for in vivo near-infrared photothermal cancer therapy. ACS Applied Materials & Interfaces. 2014;**6**:5657-5668. DOI: 10.1021/am5001823

[76] Li KC, Chu HC, Lin Y, Tuan HY, Hu YC. PEGylated copper nanowires as a novel photothermal therapy agent. ACS Applied Materials & Interfaces. 2016;**8**:12082-12090. DOI: 10.1021/acsami.6b04579

[77] Ruff J, Steitz J, Buchkremer A, Noyong M, Hartmann H, Besmehn A, Simon U. Multivalency of PEG-thiol ligands affects the stability of NIR-absorbing hollow gold nanospheres and gold nanorods. Journal of Materials Chemistry B. 2016;**4**:2828-2841. DOI: 10.1039/c6tb00674d

[78] Hone DC, Walker PI, Evans-Gowing R, FitzGerald S, Beeby A, Chambrier I, Cook MJ, Russell DA. Generation of cytotoxic singlet oxygen via phthalocyanine-stabilized gold nanoparticles: A potential delivery vehicle for photodynamic therapy. Langmuir. 2002;**18**:2985-2987. DOI: 10.1021/la0256230

[79] Connor EE, Mwamuka J, Gole A, Murphy CJ, Wyatt MD. Gold nanoparticles are taken up by human cells but do not cause acute cytotoxicity. Small. 2005;**1**:325-327. DOI: 10.1002/smll.200400093

[80] Liu YL, Shipton MK, Ryan J, Kaufman ED, Franzen S, Feldheim DL. Synthesis, stability, and cellular internalization of gold nanoparticles containing mixed peptide-poly(ethylene glycol) monolayers. Analytical Chemistry. 2007;**79**:2221-2229. DOI: 10.1021/ac061578f

[81] Blättler TM, Pasche S, Textor M, Griesser HJ. High salt stability and protein resistance of poly(L-lysine)-g-poly(ethylene glycol) copolymers covalently immobilized via aldehyde plasma polymer interlayers on inorganic and polymeric substrates. Langmuir. 2006;**22**:5760-5769. DOI: 10.1021/la0602766

[82] Paciotti GF, Kingston DGI, Tamarkin L. Colloidal gold nanoparticles: A novel nanoparticle platform for developing multifunctional tumor-targeted drug delivery vectors. Drug Development Research. 2006;**67**:47-54. DOI: 10.1002/ddr.20066

[83] Cheng Y, Samia AC, Meyers JD, Panagopoulos I, Fei B, Burda C. Highly efficient drug delivery with gold nanoparticle vectors for *in vivo* photodynamic therapy of cancer. Journal of the American Chemical Society. 2008;**130**:10643-10647. DOI: 10.1021/ja801631c

[84] Tan JS, Butterfield DE, Voycheck CL, Caldwell KD, Li JT. Surface modification of nanoparticles by PEO/PPO block copolymers to minimize interactions with blood components and prolong blood circulation in rats. Biomaterials. 1993;**14**:823-833. DOI: 10.1016/0142-9612(93)90004-L

[85] Klibanov AL, Maruyama K, Torchilin VP, Huang L. Amphipathic polyethyleneglycols effectively prolong the circulation time of liposomes. FEBS Letters. 1990;**268**:235-237. DOI: 10.1016/0014-5793(90)81016-H

[86] Petros RA, DeSimone JM. Strategies in the design of nanoparticles for therapeutic applications. Nature Reviews. Drug Discovery. 1999;**9**:615-627. DOI: 10.1038/nrd2591

[87] Jokerst JV, Lobovkina T, Zare RN, Gambhir SS. Nanoparticle PEGylation for imaging and therapy. Nanomedicine. 2011;**6**:715-728. DOI: 10.2217/nnm.11.19